A Performance Analysis of All-Optical Clock Extraction Circuit Based on Stimulated Brillouin Scattering

Xiang Zhou, *Member, IEEE*, Hossam H. M. Shalaby, *Senior Member, IEEE*, Lu Chao, *Member, IEEE*, T. H. Cheng, *Member, IEEE*, and Peida Ye, *Fellow, IEEE*

***Abstract*—In this paper, we develop an analytical method to deal with the timing performance in an optical clock extraction circuit based on stimulated Brillouin scattering (SBS). Three kinds of SBS active filters are considered and their frequency-transfer functions are obtained under the assumption that pump depletion caused by SBS is negligible. When pump depletion is taken into account, an SBS active filter acts as a nonlinear filter. To investigate the timing performance at this situation, we introduce the concept of "dynamic frequency-transfer function" to describe its frequency-response property for a fixed-signal light and pump light. Using the obtained "frequency-transfer function," we give analytical expressions for both root-mean-square (rms) phase jitter and rms amplitude jitter of the extracted optical clock, in which we have taken the impacts of SBS gain, pump light linewidth, optical pulse chirp, and pump detuning into account. Finally, a detailed numerical investigation on the timing performance for the three active filters is presented.**

***Index Terms*—All-optical signal processing, optical active filter, optical clock extraction, optical tank circuit, rms amplitude jitter, root-mean-square (rms) phase jitter, stimulated Brillouin scattering (SBS).**

I. Introduction

THERE is a growing demand for very-high-speed data transmission and processing systems, that exceed the speed limit of conventional electronic circuits. All-optical signal processing is the most promising scheme to achieve such system because of its potential of ultrahigh-speed response.

System synchronization is one of the serious problems in constructing all-optical signal processing systems, such as all-optical regenerative repeaters, all-optical time-division switching systems, and all-optical demultiplexers. In order to realize the system synchronization, an all-optical clock extraction circuit, which recovers a timing information from an incoming optical data stream and produces an optical clock without an intermediate electric stage is required.

Up to the present, several optical timing extraction techniques suitable for high-speed operations have been demonstrated, some examples include inject-locking of a mode-locked laser [1], [2], optical phase-lock loop (PLL) [3], [4], optical passive tank circuit based on Fabry–Perot resonator [5], [6], and optical active tank circuit based on stimulated Brillouin scattering (SBS) [7]–[9]. Each of these methods has advantages and drawbacks. For the mode-locked laser, high-quality clock can be recovered, however, when setting up the laser the cavity length must be tuned carefully. For optical PLL, extremely stable operation is obtainable but such a technique is very complex and more suitable for clock extraction at the frame rate. Compared with the previous two methods, optical passive tank circuit based on Fabry–Perot resonator has the advantages of ultrahigh-speed operation and simple configuration due to its passive structure. For this circuit, however, it is impossible to independently control the center frequency of each passband and the free-spectral range (FSR). Consequently, there exists a tradeoff between the carrier frequency control and the FSR variation of the resonator, also carrier frequency variation will introduce a phase wander in the extracted optical clock [10]. To overcome some of these drawbacks, an active optical tank circuit based on the comb-shaped gain spectrum generated by a Brillouin amplifier was proposed and demonstrated [7]–[9]. In [7], Kawakami *et al.* use several continuous-wave (CW) lights with different center frequencies as pumps to amplify multiple clock-related line spectral components of the optical data signal. In their systems, the center frequency of each pump light can be tuned separately; as a result, absolute-gain band frequency and FSR can be independently controlled. In [8], Butler *et al.*directly use the comb spectral components of the signal light as the pump lights. In this scheme, the clock can be recovered in optical domain without the knowledge of the incoming data bit rate, moreover, it can also be used for multiwavelength all-optical clock recovery, as was shown in [9].

In this paper, we present an analytical study on the timing performance of the active optical tank circuit based on SBS. To our knowledge, this is the first time this issue is being dealt with. Through the classical parameter-coupling model of stimulated scattering, we find that an SBS active filter acts as a linear filter when pump depletion cased by SBS is negligible. Based on this, we obtain its frequency-transfer function. When pump depletion cased by SBS cannot be neglected, an SBS active filter becomes a nonlinear filter. To investigate the timing performance at this instance, we introduce the concept of "dynamic frequency-transfer function" to describe its frequency-response property for a fixed signal light and pump light. Then, by using the obtained "frequency-transfer function," we give analytical expressions for both root mean square (rms) phase jitter and rms amplitude jitter of the extracted optical clock. Using these formulas, we present a detailed numerical investigation

Manuscript received March 28, 2000.

X. Zhou, H. H. M. Shalaby, L. Chao, and T. H. Cheng are with the School of Electrical and Electronic Engineering, Nanyang Technological University, Singapore 639798.

P. Ye is with the Beijing University of Posts and Telecommunications, The Office of President, Beijing, 100876, China.

Publisher Item Identifier S 0733-8724(00)09096-4.

on the impacts of SBS gain, SBS gain bandwidth, pump light linewidth, optical-pulse frequency chirp, and pump detuning on the timing performance.

The remainder of our paper is organized as follows. Section II is devoted to the basic description of the principle of the active optical tank circuit. The derivation of the "frequency transfer function" for SBS active filter is given in Section III. In Section IV, we present the analytical expressions for rms phase jitter and rms amplitude jitter of the extracted optical clock. In Section V, we give the numerical results and discussions. The conclusions are presented in the last section.

II. Principle of Optical Active Tank Circuit

In general, the optical field of a random return to zero (RZ) intensity modulation (IM) data stream can be described as

$$e_i(t) = \sum_{k=-\infty}^{\infty} a_k u(t - kT_c) e^{j2\pi f_0 t} \tag{1}$$

where $u(t)$ represents the complex envelope of the optical pulse, T_c is data clock period, a_k takes the unipolar values 0, 1 with equal probability in the interval $[kT_c, (k+1)T_c]$, and f_0 is the center frequency of the carrier. For simplicity, carrier phase noise and other optical noise are ignored. Using Fourier transformation, (1) can be expressed as

$$\begin{aligned} e_i(t) &= A(t) + B(t) \\ A(t) &= \sum_{k=-\infty}^{\infty} A_n \exp[j2\pi(f_0 + kf_c)t + \phi_k] \\ B(t) &= \int_{-\infty}^{\infty} B(p) \exp[j2\pi(f_0 + pf_c)t + \phi(p)]\, dp \\ & \qquad (p \text{ is not an integer}) \end{aligned} \tag{2}$$

where f_c denotes the data clock frequency. It can be observed that the envelope of $A(t)$ is periodic with frequency f_c. This suggests that $A(t)$ can be used as the clock signal. Note that $A(t)$ [or $B(t)$] is a series (or integration) of optical frequency components, and they can be amplified or suppressed using nonlinear optical effects or optical devices. The passive optical tank circuit in [5] corresponds to the case that suppresses $B(t)$ and the active optical tank circuit corresponds to another situation that amplifies multiple frequency components which are included in $A(t)$.

The Brillouin amplifier in optical fibers has a highly efficient nonlinear optical effect with which large gains can be achieved using a counter propagating pump light. The frequency of the Brillouin gain is lower than the pump light's frequency, and this frequency offset is called Stokes shift. The Stokes shift is proportional to the pump light frequency given as [11]

$$f_B = 2\nu_A f_p n/c \tag{3}$$

where n is the refractive index, ν_A is the acoustic velocity, and f_p means the pump light frequency. In single-mode silica fibers at 1.55 μm, f_B is approximately 11 GHz, and the Brillouin scattering line width is 10 to 100 MHz dependeding on the types of fiber [12]. In high-speed optical transmission systems that exceed 2 to 3 Gbs/s, the data stream's spectrum is spread out much more than the Brillouin gain bandwidth, therefore, we can use the comb-pumped gain spectrum generated by several pump lights to selectively amplify multiple-frequency components which are included in $A(t)$ as shown in Fig. 1.

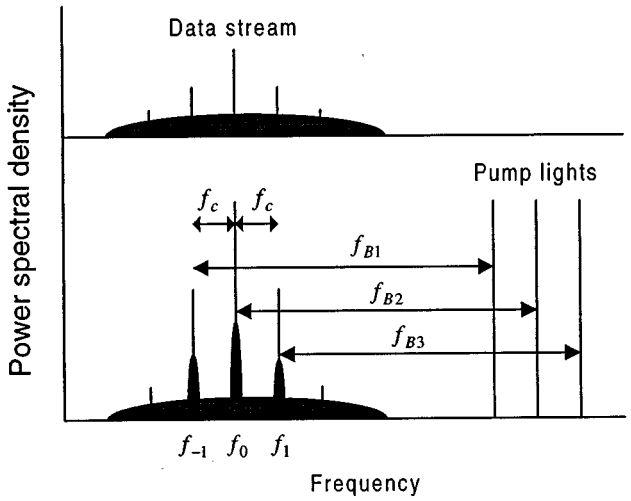

Fig. 1. Schematic illustration for SBS active optical tank circuit. f_{B1}, f_{B2}, and f_{B3} denote Stokes shifts corresponding to the three pump lights, respectively.

In the reported demonstration experiments, the comb gain spectrum was obtained in three manners. The first method employs two independent CW lights as the pumps to generate gain spectrum at f_0 and $f_0 + f_c$ [7]. The second method uses three line spectral components of a sinusoidal phase-modulated CW light as the pumps to amplify the signal spectral components at $f_0 - f_c$, f_0, and $f_0 + f_c$ [7]. The third method directly uses the line spectral components of the incoming signal as the pumps [8], [9].

For the preceding two methods, the CW lights are offset locked to the signal by automatic frequency control (AFC) (fixed-frequency offsets are utilized, for automatic modification of frequency offset is difficult), and the power of each pump is tunable. Note that Brillouin shift is dependent on pump light frequency, it is then immediate that both the signal light frequency variation and nonideal AFC will introduce pump detuning. If we use Δf_s to represent signal-light-frequency variation-induced pump detuning and df express nonideal AFC-induced pump detuning, it is clear that Δf_s should be identical for all the pumps but df is dependent on the configuration of SBS amplifier. For the first method, the two pumps are controlled independently, their detuning frequencies will be different. For the second method, three pumps are generated from one CW light, obviously they should have exactly the same detuning frequency.

The third method splits the incoming signal light into two unequal beams. The larger beam, named $I_1(t)$, is used as the pump light; the other beam, named $I_2(t)$, is modulated at a frequency which is identical to the Brillouin shift by a modulator, so that some of its energy is down-shifted to the Brillouin resonant frequency. Thus the comb gain spectrum generated by the line spectral components of $I_1(t)$ can be utilized to amplify the corresponding down-shifted spectral components in $I_2(t)$ (we

denote the down-shifted part as $I_2^d(t)$ hereafter). Unlike the previous two methods, it can be noted that the pumps have unequal powers and they cannot be controlled independently, in addition, the pump power will fluctuate with data pattern. Therefore, the basic requirement for this scheme is that the SBS amplifier must be fully saturated. If the amplifier is unsaturated, a small amount of noise can create substantial amplitude variation in the recovered clock because of the exponential nature of gain, besides, the baseband dc component in $I_2^d(t)$ will see much larger gain than the baseband clock components, as a result, the dc component in the recovered clock will be rather strong. However, when SBS amplifier is fully saturated, the baseband clock and dc components in $I_2^d(t)$ will see approximately the same gain. This can be shown as follows.

Let $I_p(z)$ express the optical intensity of a monochromatic CW pump and $I_s(z)$ denote the light intensity of the corresponding monochromatic CW signal. Assuming that the signal light is launched into the fiber at $z = 0$ and travels to the receiver at $z = L$ and the pump light is fed back down the fiber from the receiver, we have $dI_s(z)/dz = g_B I_p(z) I_s(z) - \alpha I_s(z)$ [13]. Here α is the attenuation constant and g_B is the Brillouin-gain coefficient. When SBS gain is fully saturated, i.e., $dI_s(z)/dz|_{z=0} \to 0$, we get $I_p(0) \to \alpha/g_B$ and we can give the saturated SBS power gain as

$$G_s \approx \left[I_p(L) - \frac{\alpha}{g_B} \right] \frac{1}{I_s(0)} + 1. \tag{4}$$

Typically, we have $\alpha = 0.057$ (i.e., 0.25 dB), $g_B = 5 \times 10^{-11}$ m/W, and $A_{\text{eff}} = 50\ \mu\text{m}^2$ (A_{eff} denotes the effective core area of the fiber). Let $P_s(0) = I_s(0) A_{\text{eff}}$, $P_p(L) = I_p(L) A_{\text{eff}}$, then it can been seen, so long as $P_s(0) > 0.0057$ mW, we get $\alpha/(g_B I_s(0)) < 10$. For successful clock extraction, $I_p(L)/I_s(0)$ should be much greater than 10, then we can directly write G_s as $I_p(L)/I_s(0)$. In our optical tank circuit, $I_p(L)/I_s(0)$ is constant for various line spectral components in $I_2^d(t)$. It is obvious that those whose power is large enough will see equal gain. In the case when optical pulse chirp is not too large, or optical pulse is not too narrow, only baseband dc and harmonics of the first order have enough power to obtain a large gain. Therefore, we can deal with it as a three-pump clock extraction.

Unlike the previous two schemes, this circuit does not need AFC, moreover, it is bit-transparent. For this scheme, however, signal-light frequency variation will also introduce pump detuning if the modulation frequency f_B used to down-shift the signal light is designed to be a fixed value. In addition, there exist an inherent pump detuning in such a circuit. Note that the three pumps have frequencies of $f_0 - f_c$, f_0, and $f_0 + f_c$, and accordingly the down-shifted signal light have line spectral components of $f_0 - f_c - f_B$, $f_0 - f_B$, and $f_0 + f_c - f_B$. It is easily seen that at most only one pump can be tuned to be the ideal value of frequency. Usually, we set f_B as the Stokes shift of the pump at frequency f_0.

Fig. 2(a)–(c) gives the schematic illustration of the gain spectrum profiles for the three methods, respectively, where solid lines denote the cases without pump detuning and the dashed lines denote the cases with pump detuning. In Fig. 2(a) and (b), pump depletion is neglected and each pump is assumed to have equal power. In Fig. 2(c), the SBS gain is assumed to be fully saturated.

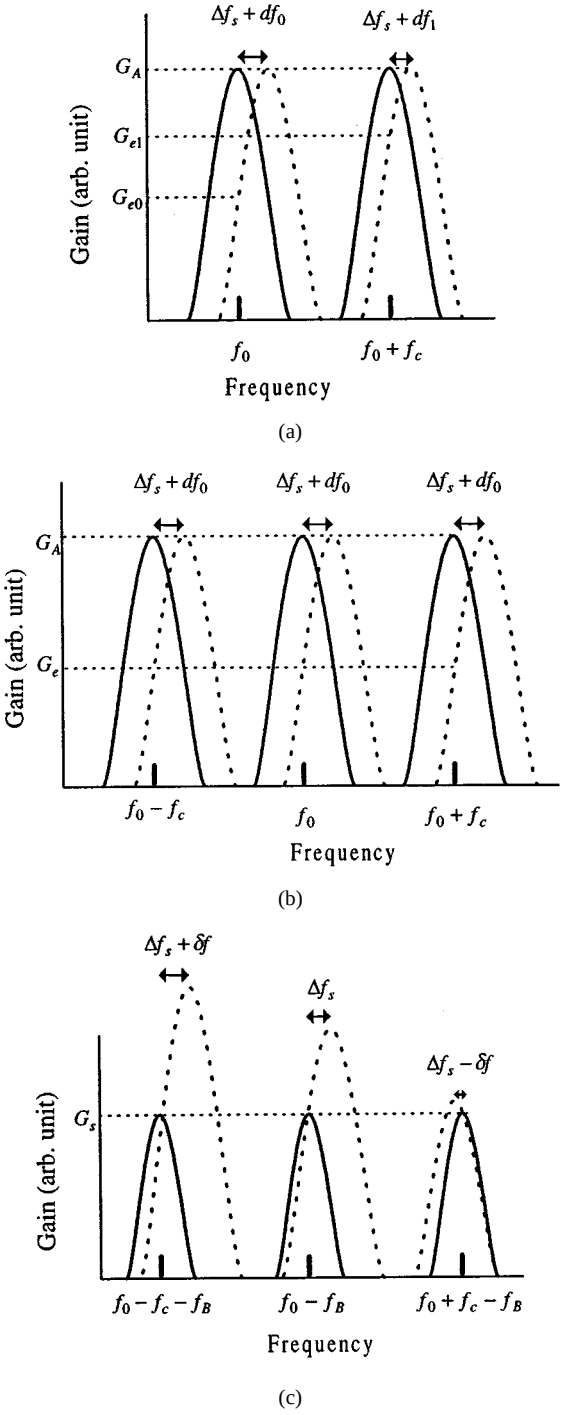

Fig. 2. Schematic illustration of SBS gain spectrum profiles. (a) The case that employ two independent CW lights as the pumps. (b)The case that utilizes a phase-modulated CW light as the pumps. (c) The case that directly uses the incoming signal as the pumps. Δf_s, df, and δf represent the pump detuning caused by signal-light frequency variation, nonideal AFC, and the inherent pump detuning, respectively.

III. Frequency-Transfer Function of SBS Active Filter

In the previous section, we have shown that pump detuning is inevitable for an SBS active optical tank circuit. Note that

this circuit cannot suppress undesirable frequency components $B(t)$ in (2), unlike the ordinary cavity, therefore, $B(t)$ will impose a detrimental impact on the extracted optical clock with finite Brillouin gain. In addition, the nonzero gain width, pump-lights linewidth, and signal-light linewidth may also degrade the timing performance. To investigate their impact, we need to know the frequency-transfer function of this circuit.

A. Without Pump Depletion

Let us consider an SBS amplifier with only one pump. Similarly to the above section, we assume that the signal light is launched into the fiber at $z = 0$ and travels to the receiver at $z = L$ and the pump light is fed back down the fiber from the receiver. Here we take the pump linewidth into account, but still neglect the signal-light linewidth, also, we assume that the pump depletion caused by stimulated light scattering is negligible. Following the classical parametric-coupling model of stimulated scattering [14], we obtain the following two coupled equations:

$$\frac{\partial E_s(z)}{\partial z} = -\left(jK_1K_2I_p(z)\int_{-\infty}^{\infty}\frac{P(f_p)}{\Delta\Omega - j\Gamma}df_p + \frac{\alpha}{2}\right)E_s(z) \tag{5}$$

$$\frac{\partial I_p(z)}{\partial z} = \alpha I_p(z) \tag{6}$$

where $E_s(z)$ is the slowly varying amplitude of the Stokes field, and $I_p(z)$ denotes the intensity of the pump light. The frequency-dependent denominator in (5) is a consequence of Kramers–Kronig dispersion relations [14]. Γ^{-1} is the acoustic phonon lifetime resulting in a spontaneous Brillouin scattering linewidth of $\Delta\nu_B = 2\Gamma$ [full-width at half-maximum (FWHM), in hertz]. $P(f_p)$ denotes the power spectral density of the pump light source and K_1 and K_2 are coupling constants given by

$$K_1 = K_2\frac{\rho_o n^2 \varepsilon_o}{2\nu_A} \tag{7}$$

$$K_2 = \frac{n^3\rho_{12}f_s}{2c\rho_o}\,(\hat{e}_p, \hat{e}_s) \tag{8}$$

where ρ_0 is the average material density, n is the refractive index, ε_0 is the free-space permitivity, ν_A is the acoustic velocity, ρ_{12} is the longitudinal elastic-optic coefficient, and c is the vacuum speed of light. The unit vectors $\hat{e}_p$ and $\hat{e}_s$ are in the directions of the optical fields. The factor $\Delta\Omega = f_p - f_s - f_B$ describes the detuning from the SBS gain line center, where f_p, f_s, and f_B denote the pump-light frequency, signal-light frequency, and the Stokes shift, respectively. f_B is related to f_p as (3). From (5) and (6), we obtain

$$E_s(L) = E_s(0)\exp\left[\frac{1}{2}\left(g_{B0}I_p(L)L_e\Gamma^2 \cdot\int_{-\infty}^{\infty}\frac{p(f_p)}{\Delta\Omega^2+\Gamma^2}df_p - \alpha L\right) - j\Phi\right] \tag{9}$$

where g_{B0} is the Brillouin-gain coefficient at the line center

$$g_{B_o} = \frac{2K_1K_2r}{\Gamma} \tag{10}$$

r is the integrated average of $(\hat{e}_p\cdot\hat{e}_s)^2$ and takes the value of $2/3$ for long lengths of nonpolarization-preserving fiber and 1 for polarization preserving fiber [15], L_e is the effective interaction length, given as $L_e = [1 - \exp(-\alpha L)]/\alpha$, and Φ (radians) represents the nonlinear phase shift

$$\Phi = \frac{g_{B_o}I_p(L)L_e\Gamma}{2}\int_{-\infty}^{\infty}\frac{\Delta\Omega P(f_p)}{\Delta\Omega^2+\Gamma^2}df_p. \tag{11}$$

From the above, it is clear that an SBS amplifier (without pump depletion) can be viewed as a linear time-invariable filter and its frequency transfer function can be easily derived from (9). Then, we can get the baseband frequency transfer function for optical tank circuit with two pumps and three pumps as

$$\vec{H}(f) = \sum_{k=0}^{1}H_k(f - kf_c - \Delta f_k) + 1 \tag{12}$$

and

$$\vec{H}(f) = \sum_{k=-1}^{1}H_k(f - kf_c - \Delta f_k) + 1 \tag{13}$$

respectively, where

$$H_k(f) = \exp\left[\frac{g_{B0}I_kL_e}{2}\int_{-\infty}^{\infty}\frac{p_b^k(f_p)}{(f_p - f)^2+\Gamma^2} \cdot[\Gamma^2 - j\Gamma(f_p - f)]df_p\right] - 1. \tag{14}$$

Δf_k, I_k, and $P_b^k(f_p)$ denote the pump detuning, the initial pump light intensity, and the baseband power spectral density, corresponding to the kth-pump light source. In the above three equations, the loss term $\exp(-\alpha L/2)$ has been ignored, since it has no impact on the timing performance apart from the power loss.

B. With Pump Depletion

Now let us consider the case when pump depletion by SBS cannot be neglected. In this situation, the SBS gain depends not only on pump light but also on signal light and the SBS amplifier acts as a nonlinear filter. Strictly speaking, the concept of frequency transfer function is unsuitable for a nonlinear system. To investigate the timing performance in such a case, we introduce a concept of "dynamic frequency transfer function." Let $\vec{E}_s^{\,\text{in}}(f)$, $\vec{E}_s^{\,\text{out}}(f)$ represent the frequency-domain expressions of the input signal field and the output signal field, respectively, then we define the function $H_d(f) = \vec{E}_s^{\,\text{out}}(f)/\vec{E}_s^{\,\text{in}}(f)$ as "dynamic frequency transfer function." To obtain $H_d(f)$, we divide the fiber length into a number of segments of width l as shown in Fig. 3. Within a segment, we can neglect pump depletion and take pump intensity as the value in the middle. For one-pump Brillouin amplifier, assuming that the pump-light linewidth is negligible, based on (9) and through an iterative process, we can obtain

$$\vec{E}_s^{\,\text{out}}(f) = \vec{E}_s^{\,\text{in}}(f)\exp\left[\frac{1}{2}\left(g_{B0}I_eL_e\frac{(\Gamma^2 - j\Gamma\Delta\Omega)}{\Delta\Omega^2+\Gamma^2} - \alpha L\right)\right] \tag{15}$$

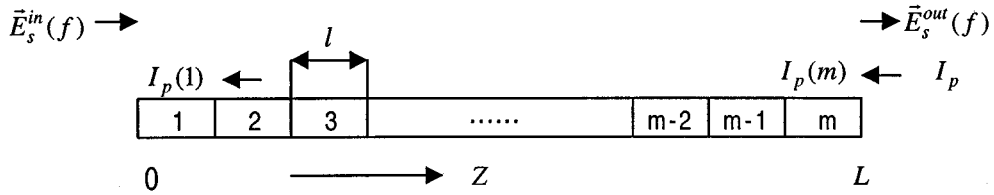

Fig. 3. Schematic illustration of a split-step method used for "dynamic frequency transfer function" deduction. $I_p(n)$ is the pump light intensity at the middle of the nth segment.

where

$$I_e = \sum_{n=1}^{m} \frac{l_e}{L_e} |I_p(n)|^2 \tag{16}$$

$\Delta\Omega = f_p - f - f_B$, $l_e = (1 - \exp(-\alpha l))/\alpha$, and $I_p(n)$ denotes the pump light intensity in the middle of the nth segment. Note that (15) can be obtained directly from (9) by replacing $I_p(L)$ with I_e in the case of negligible pump linewidth. Hence, I_e can be viewed as the effective pump optical intensity. When the number of segments m is very large, we have $l_e \approx l$ and the sum in (16) becomes an integration

$$I_e = \int_0^L \frac{I_p(z)}{L_e} dz. \tag{17}$$

Note that in our optical tank circuit $\vec{E}_s^{\text{in}}(f)$ consists of a continuos spectral component and a line spectral component (corresponding to one pump). So long as the pump detuning is not too large, the impact of the continuous spectral component on the pump depletion is negligible. In this case, $I_p(z)$ can be obtained analytically [13] as

$$I_p(z) = \frac{(1-b)\Pi(z,b)}{\Pi(z,b) - b} I_p(L) \exp(-\alpha L + \alpha z) \tag{18}$$

where

$$\Pi(z,b) = \exp\left\{\frac{1}{\alpha}[1 - \exp(-\alpha L + \alpha z)](1-b) g_B(\Delta f) I_p(L)\right\} \tag{19}$$

$$b = I_s(L)/I_p(L) \tag{20}$$

$$g_B(\Delta f) = \frac{g_{B_o}\Gamma^2}{\Delta f^2 + \Gamma^2}. \tag{21}$$

In the above equations, Δf denotes the pump detuning and $I_s(L)$ expresses the intensity of the output signal light line spectral component. Let $d = I_s(0)/I_p(L)$ ($I_s(0)$ is the intensity of the input signal line spectral component). Thus b is the solution of

$$d = \frac{(1-b)b}{\Pi(0,b) - b} \exp(-\alpha L). \tag{22}$$

From the above discussion, we can see that I_e is dependent not only on input pump-light intensity, but also on input signal-light intensity and pump detuning. For a given signal-light and pump-light intensity, we can write I_e as a function of pump detuning, i.e., $I_e(\Delta f)$. Consequently, we can give the baseband form of the "dynamic frequency transfer function" for optical tank circuit with two pumps and three pumps as

$$\vec{H}_d(f) = \sum_{k=-1}^{1} H_k^d(f - kf_c - \Delta f_k, \Delta f_k) + 1 \tag{23}$$

and

$$\vec{H}_d(f) = \sum_{k=0}^{1} H_k^d(f - kf_c - \Delta f_k, \Delta f_k) + 1 \tag{24}$$

respectively, where

$$H_k^d(f, \Delta f) = \exp\left[\frac{g_{B0} L_e I_e^k(\Delta f)(\Gamma^2 + j\Gamma f)}{2(f^2 + \Gamma^2)}\right] - 1. \tag{25}$$

Here k denotes the case corresponding to the kth pump.

When SBS gain is fully saturated, the calculation for $I_e^k(\Delta f)$ can be simplified. Let G_s^k express the saturated power gain obtained by the corresponding signal line spectral component, thus

$$I_e^k(\Delta f) = \ln(G_s^k) \Big/ \left[\frac{g_{B0} L_e \Gamma^2}{\Delta f_k^2 + \Gamma^2}\right] \tag{26}$$

where $\ln(\,)$ means natural logarithm.

IV. Performance Analysis

Let $E_i(t)$ and $E_0(t)$ express the baseband form of the input-signal optical field and the output-signal optical field of the SBS active optical tank circuit, respectively, then $E_0(t)$ can be expressed as

$$E_0(t) = E_i(t) \otimes h(t) = \left[\sum_{k=-\infty}^{\infty} a_k u(t - kT_c)\right] \otimes h(t) \tag{27}$$

where $h(t)$ is the temporal response of $\vec{H}_d(f)$ (or $\vec{H}(f)$) and $\otimes$ denotes convolution integration.

A. rms Phase Jitter

1) With Three Pumps: In the case when three pumps are used (corresponding to the second and the third methods in Section II), $E_0(t)$ can be written as

$$\begin{aligned} E_0(t) &= E_i(t) \otimes \Big(h_0(t) e^{j2\pi\Delta f_0 t} + h_1(t) \exp[j2\pi(f_c + \Delta f_1)t] \\ &\qquad + h_{-1}(t) \exp[-j2\pi(f_c - \Delta f_{-1})t] + \delta(t)\Big) \\ &= B_0(t) e^{j\theta_0(t)} + B_1(t) \exp[j(2\pi f_c t + \theta_1(t))] \\ &\qquad + B_{-1}(t) \exp[-j(2\pi f_c t - \theta_{-1}(t))] + E_i(t) \end{aligned} \tag{28}$$

where $h_k(t)$ is the temporal response of $H_k^d(f, \Delta f_k)$ (or $H_k(f)$). In fact, $H_k(f)$ can be viewed as a special case of $H_k^d(f, \Delta f_k)$ if pump linewidth is neglected. $B_0(t)$, $B_1(t)$, $B_{-1}(t)$, $\theta_0(t)$, $\theta_1(t)$, and $\theta_{-1}(t)$ are real random functions.

When SBS gain is large enough, the last term in (29) is small compared to the first three terms and its contribution to phase jitter is negligible. Mathematically, we can write $B_0(t)$, $B_1(t)$, $B_{-1}(t)$, $\theta_0(t)$, $\theta_1(t)$, and $\theta_{-1}(t)$ as

$$\begin{aligned} B_1(t) &= B_1 + \Delta B(t) \\ B_0(t) &= B_0 + \Delta B_0(t) \\ B_{-1}(t) &= B_{-1} + \Delta B_{-1}(t) \\ \theta_1(t) &= \theta_1 + \Delta\theta_1(t) \\ \theta_0(t) &= \theta_0 + \Delta\theta_0(t) \end{aligned}$$

and

$$\theta_{-1}(t) = \theta_{-1} + \Delta\theta_{-1}(t)$$

where B_1, B_0, B_{-1}, θ_1, θ_0, and θ_{-1} are the statistical average of $B_1(t)$, $B_0(t)$, $B_{-1}(t)$, $\theta_1(t)$, $\theta_0(t)$, and $\theta_{-1}(t)$, respectively. Let $U(f)$ expresses the Fourier transform of $u(t)$, then it is easy to get that

$$\begin{aligned} B_1 &= \frac{1}{2}|f_c U(f_c) H_1^d(-\Delta f_1, \Delta f_1)| \\ B_0 &= \frac{1}{2}|f_c U(0) H_0^d(-\Delta f_0, \Delta f_0)| \\ B_{-1} &= \frac{1}{2}|f_c U(-f_c) H_{-1}^d(-\Delta f_{-1}, \Delta f_{-1})| \\ \theta_1 &= \arg\{U(f_c) H_1^d(-\Delta f_1, \Delta f_1)\} \\ \theta_0 &= \arg\{U(0) H_0^d(-\Delta f_0, \Delta f_0)\} \end{aligned}$$

and

$$\theta_{-1} = \arg\{U(-f_c) H_{-1}^d(-\Delta f_{-1}, \Delta f_{-1})\}$$

where $\arg\{\,\}$ means the argument of $\{\,\}$. When pump detuning is not too large, we have $B_1 \gg \Delta B_1(t)$, $B_0 \gg \Delta B_0(t)$, and $B_{-1} \gg \Delta B_{-1}(t)$. Consequently, we can get the corresponding optical intensity $|E_0(t)|^2$ as

$$\begin{aligned} |E_0(t)|^2 = {} & B_0^2 + B_1^2 + B_{-1}^2 \\ & + 2B_0 B_1 \cos(2\pi f_c t + \theta_1(t) - \theta_0(t)) \\ & + 2B_0 B_{-1} \cos(2\pi f_c t - \theta_{-1}(t) + \theta_0(t)) \\ & + 2B_1 B_{-1} \cos(4\pi f_c t + \theta_1(t) - \theta_{-1}(t)) \\ & + \text{small term.} \end{aligned} \tag{29}$$

First, let us consider the case where pump lights are generated by a phase-modulated CW light. In this case we have $\Delta f_0 = \Delta f_1 = \Delta f_{-1}$. Assuming that $u(t)$ is an even symmetric complex function (including chirp) and $I_e^1(\Delta f_1) = I_e^0(\Delta f_0) = I_e^{-1}(\Delta f_{-1})$, we then have $B_1 = B_{-1}$ and

$$\begin{aligned} \frac{\theta_1(t) + \theta_{-1}(t)}{2} - \theta_0(t) = {} & \arg[U(f_c)] - \arg[U(0)] \\ & + \frac{\Delta\theta_1(t) + \Delta\theta_{-1}(t)}{2} - \Delta\theta_0(t). \end{aligned} \tag{30}$$

When the optical pulse chirp is relatively small, $\arg[U(f_c)] - \arg[U(0)]$ should be small, and hence

$$\cos\left(\frac{\theta_1(t) + \theta_{-1}(t)}{2} - \theta_0(t)\right) \approx 1.$$

As a result, (29) can be rewritten as

$$\begin{aligned} |E_0(t)|^2 = {} & \left[B_0 + 2B_1 \cos\left(2\pi f_c t + \frac{\theta_1(t) - \theta_{-1}(t)}{2}\right)\right]^2 \\ & + \text{small term.} \end{aligned} \tag{31}$$

It can be observed that $[\theta_1(t) - \theta_{-1}(t)]/2$ just characterizes the phase of the extracted optical clock. When pump linewidth is taken into account but neglecting pump depletion, (31) is still valid so long as all the pumps have equal powers.

Next we consider the case when pump lights are generated directly from the signal. In this situation, we have $\Delta f_0 = \Delta f_s$, $\Delta f_1 = \Delta f_s - \delta f$, and $\Delta f_{-1} = \Delta f_s + \delta f$ (δf is the inherent pump detuning and Δf_s is signal-carrier-frequency variation-induced detuning). Assume that the gain–length product of the SBS amplifier is large enough to make SBS gain tend to be saturated even when pump detuning is relatively large. From (25) and (26), we can get B_1, B_0, B_{-1}, θ_1, θ_0, and θ_{-1} as

$$B_k = f_c |U(k f_c)| G_s^k \qquad (k = 1, 0, -1) \tag{32}$$

$$\theta_k = \frac{\Delta f_k}{\Gamma} \ln G_s^k + \arg[U(k f_c)] \qquad (k = 1, 0, -1). \tag{33}$$

From Section II we know that $G_s^1 = G_s^0 = G_s^{-1}$, and it is immediate that (30) and (31) are still valid for this case.

Thus the normalized rms phase jitter for both cases can be expressed as

$$\sigma_J = \frac{1}{4\pi}\sqrt{\langle[\Delta\theta_1(t) - \Delta\theta_{-1}(t)]^2\rangle} \tag{34}$$

where $\langle\,\rangle$ means statistical average. From (28), we get

$$\begin{aligned} & B_1(t)\cos(2\pi f_c t + \Delta\theta_1(t)) \\ & \quad = \mathrm{Re}\{(E_i(t) \otimes (h_1(t)\exp[j2\pi(f_c + \Delta f_1)t]))e^{-j\theta_1}\} \end{aligned} \tag{35}$$

$$\begin{aligned} & B_{-1}(t)\cos(2\pi f_c t - \Delta\theta_{-1}(t)) \\ & \quad = \mathrm{Re}\{(E_i(t) \otimes (h_{-1}(t)\exp[-j2\pi(f_c - \Delta f_{-1})t]))e^{j\theta_{-1}}\} \end{aligned} \tag{36}$$

where $\mathrm{Re}\{\,\}$ means the real part of $\{\,\}$. At the time instant $t_n = (2n+1)/(4f_c)$ (n is an integer), we have

$$\begin{aligned} & B_1(t)\sin(\Delta\theta_1(t_n)) \\ & \quad = \mathrm{Re}\{(E_i(t) \otimes (h_1(t)\exp[j2\pi(f_c + \Delta f_1)t]))e^{-j\theta_1}\}_{t=t_n} \end{aligned} \tag{37}$$

$$\begin{aligned} & B_{-1}(t)\sin(\Delta\theta_{-1}(t)) \\ & \quad = \{(E_i(t) \otimes (h_{-1}(t)\exp[-j2\pi(f_c - \Delta f_{-1})t]))e^{j\theta_{-1}}\}_{t=t_n}. \end{aligned} \tag{38}$$

Note that $\Delta\theta_1(t_n)$ and $\Delta\theta_{-1}(t_n)$ are very small and it is clear that $\sin(\Delta\theta_1(t_n)) \approx \Delta\theta_1(t_n)$ and $\sin(\Delta\theta_{-1}(t_n)) \approx \Delta\theta_{-1}(t_n)$. Then we get

$$\begin{aligned} & \Delta\theta_1(t_n) - \Delta\theta_{-1}(t_n) \\ & \quad \approx -\frac{1}{B_1}\mathrm{Re}\{(E_i(t) \otimes (h_1(t) \\ & \qquad \cdot \exp[j2\pi(f_c + \Delta f_1)t]))e^{-j\theta_1}\}_{t=t_n} \\ & \qquad - \frac{1}{B_{-1}}\mathrm{Re}\{(E_i(t) \otimes (h_{-1}(t) \\ & \qquad \cdot \exp[-j\pi(f_c - \Delta f_{-1})t]))e^{j\theta_{-1}}\}_{t=t_n}. \end{aligned} \tag{39}$$

Thus it is easy to obtain

$$\sigma_J = \frac{1}{4\pi}\sqrt{(D_1 + D_{-1} + D_2)}$$
$$D_1 = \frac{f_c\{PP_1(0) - |P_1(2f_c)|\cos(\vartheta_1 - 2\theta_1)\}}{8B_1^2}$$
$$D_{-1} = \frac{f_c\{PP_{-1}(0) - |P_{-1}(-2f_c)|\cos(\vartheta_{-1} + 2\theta_{-1})\}}{8B_{-1}^2}$$
$$D_2 = \frac{\begin{array}{c} f_c\{|PQ(0)|\cos(\vartheta_q - \theta_1 + \theta_{-1}) \\ -|PG(2f_c)|\cos(\vartheta_G - \theta_1 - \theta_{-1})\}\end{array}}{4B_1B_{-1}} \quad (40)$$

where

$$\begin{aligned} Q_1(f) &= U(f)H_1^d(f - f_c - \Delta f_1, \Delta f_1) \\ Q_{-1}(f) &= U(f)H_{-1}^d(f + f_c - \Delta f_{-1}, \Delta f_{-1}) \\ P_1(f) &= Q_1(f) \otimes Q_1(f) \\ P_{-1}(f) &= Q_{-1}(f) \otimes Q_{-1}(f) \\ PP_1(f) &= Q_1(f) \otimes Q_1^*(-f) \\ PP_{-1}(f) &= Q_{-1}(f) \otimes Q_{-1}^*(-f) \\ PQ(f) &= Q_1(f) \otimes Q_{-1}(f) \\ PG(f) &= Q_1(f) \otimes Q_{-1}^*(-f) \\ \vartheta_1 &= \arg[P_1(2f_c)] \\ \vartheta_{-1} &= \arg[P_{-1}(2f_c)] \\ \varphi_q &= \arg[PQ(0)] \end{aligned}$$

and

$$\varphi_G = \arg[PG(2f_c)].$$

2) With Two Pumps: In the case when two independent CW lights are used as the pumps, the optical intensity of the extracted clock is given as

$$\begin{aligned} |E_0(t)|^2 &= B_0^2(t) + B_1^2(t) \\ &\quad + 2B_0(t)B_1(t)\cos(2\pi f_c t + \theta_1(t) - \theta_0(t)). \end{aligned} \quad (41)$$

We can see that $\theta_1(t) - \theta_0(t)$ characterizes the clock phase. Based on similar deduction as given above, the normalized rms phase jitter is given by

$$\sigma_J = \frac{1}{2\pi}\sqrt{(D_1 + D_0 + D_3)}$$
$$D_0 = \frac{f_c\{PP_0(0) - |P_0(0)|\cos(\vartheta_0 - 2\theta_0)\}}{8B_0^2}$$
$$D_3 = \frac{\begin{array}{c} f_c\{|PQ_0(f_c)|\cos(\varphi_r - \theta_1 - \theta_0) \\ -|PG_0(f_c)|\cos(\varphi_s - \theta_1 + \theta_0)\}\end{array}}{4B_1B_0} \quad (42)$$

where

$$\begin{aligned} Q_0(f) &= U(f)H_1^d(f, \Delta f_0) \\ P_0(t) &= Q_0(f) \otimes Q_0(f) \\ PP_0(f) &= Q_0(f) \otimes Q_0^*(-f) \\ PQ_0(f) &= Q_1(f) \otimes Q_0(f) \\ PG_0(f) &= Q_1(f) \otimes Q_0^*(-f) \\ \vartheta_1 &= \arg[P_1(2f_c)] \\ \vartheta_0 &= \arg[P_0(0)] \\ \varphi_r &= \arg[PQ_0(f_c)] \end{aligned}$$

and

$$\varphi_s = \arg[PG_0(f_c)].$$

B. rms Amplitude Jitter

In general, the extracted optical clock (in the optical intensity form) can be written as

$$I_c(t) = [1 + a(t)]\sum_{n=-\infty}^{\infty} g(t - nT_c - J(t)) \quad (43)$$

where $a(t)$, $J(t)$, and $g(t)$ denote the normalized optical intensity variation, the timing fluctuation, and the average optical clock pulse intensity envelope, respectively. The power spectral density of $I_c(t)$ can be approximately given as [16], [17]

$$\begin{aligned} S_I(f) \cong f_c^2 \sum_{n=-\infty}^{\infty} |G(nf_c)|^2 [S_a(f - nf_c) \\ + 4\pi^2 n^2 f_c^2 S_J(f - nf_c) + \delta(f - nf_c)] \end{aligned} \quad (44)$$

where $S_a(f)$ and $S_J(f)$ denote the power spectral density of $a(t)$ and $J(t)$, respectively, and $G(f)$ is the Fourier transform of $g(t)$. The normalized rms amplitude jitter σ_A and normalized rms phase jitter σ_J of the extracted optical clock can then be expressed as

$$\sigma_A = \sqrt{\langle a^2(t)\rangle} = \sqrt{\int_{-\infty}^{\infty} S_a(f)\, df} \quad (45)$$

and

$$\sigma_J = f_c\sqrt{\int_{-\infty}^{\infty} S_J(f)\, df} \quad (46)$$

respectively.

Theoretically, the power spectral density of the extracted optical clock can be calculated as long as the frequency-transfer function of the optical tank circuit is known. Let $S_I^c(f)$ express the obtained continuous power spectral density component of the extracted optical clock, and $\sum_{n=-\infty}^{\infty} S_I^d(nf_c)\delta(f - nf_c)$ express the discrete power spectral density component. Using (44)–(46) σ_A is given as

$$\sigma_A = \sqrt{\frac{\int_{-\infty}^{\infty} S_I^c(f)\, df - \sum_{-\infty}^{\infty} 4\pi^2 n^2 \sigma_J^2 S_I^d(nf_c)}{\sum_{-\infty}^{\infty} S_I^d(nf_c)}} \quad (47)$$

According to classical Weiner theorem [18], the power spectral density of the extracted clock can be expressed as

$$S_I(f) = FT_\tau\left[\frac{1}{T_c}\int_{-(T_c/2)}^{T_c/2} R_{I,I}(t, \tau)\, dt\right] \quad (48)$$

where $R_{I,I}(t, \tau)$ means the autocorrelation function of $I_c(t)$ and $FT_\tau[\,]$ means the Fourier transform. Let $\eta = f/f_c$, then

the power spectral density is approximately given as

$$S_d(\eta f_c) \approx \frac{f_c^4}{16} \sum_{k_1=-\infty}^{\infty} \sum_{k_2=-\infty}^{\infty} \sum_{k_3=-\infty}^{\infty} Y(k_2,k_1) \cdot Y(k_3,-k_1)\delta(\eta-k_1) + \frac{f_c^3}{16} \sum_{k_1=-\infty}^{\infty} \sum_{k_2=-\infty}^{\infty} \{Y^*(k_2-\eta,k_1)Y(k_2,k_1) + Y(k_2+\eta,k_1)Y^*(k_2,k_1) + Y^*(-k_2,-\eta)Y^*(k_1+k_2,\eta) + Y(-k_2,\eta)Y(k_1+k_2,-\eta)\}. \quad (49)$$

The deduction process and the auxiliary functions of (49) are given in the Appendix. Based on (47), (49), and the value of σ_J, we can obtain σ_A.

V. Numerical Results and Discussion

To numerically investigate the timing performance of the active optical tank circuit, we assume that the incoming optical data pulses have Gaussian profiles

$$U(t) = \exp\left(-\frac{(1+jC)}{2}\frac{t^2}{T_0^2}\right) \quad (50)$$

where C is the linear chirp parameter, T_0 is the half width at the $1/e$ point. In this paper, we take $T_0 = T_c/(6\sqrt{\ln(2)})$, corresponding to 1/3 time slot width (FWHM). In addition, we choose the Brillouin scattering line width $\Delta\nu_B = 34$ MHz and assume that all the pump lights have the same linewidth (denoted as $\Delta\nu_p$ hereafter) and spectral profile. When there is no pump detuning (i.e., $\Delta f_k = 0$), we assume that all the pump lights generate the same gain spectrum profile with an equal line-center power gain G_A. Naturally, if pump depletion is negligible, the gain spectrum profiles for various pumps will still be identical (apart from the frequency translation) even with pump detuning. When pump detuning occurs but SBS gain is fully saturated, we assume that the saturated power gains obtained by all the needed signal line spectral components are identical and use G_s to express it.

A. The Impacts of SBS Gain

Fig. 4 gives the calculated power gain bandwidth as a function of G_A. Fig. 5(a) and (b) gives the calculated rms phase jitter σ_J and rms amplitude jitter σ_A against G_A for various signal bit rates, respectively, where we have assumed that $C = 0$, $\Delta f_k = 0$, and $\Delta\nu_p \approx 0$. From (40) and (42), we can find that, for a given G_A, σ_J should be identical for both cases when two pumps and three pumps are used so long as $\Delta f_k = 0$. This is the reason why we only give three curves in Fig. 5(a).

From Fig. 5, we can observe that both σ_J and σ_A reduce as SBS gain goes up. However, we can see that the value of σ_J can be very small for various values of G_A, but the value of σ_A can be very large if $G_A < 20$ dB (this effect is more serious for a two-pump circuit), moreover, σ_A takes almost the same value for different signal bit rates at a relatively small value of G_A. This is easy to understand, since this circuit cannot suppress the undesirable frequency component $B(t)$ in (2). When G_A is relatively small, the amplitude noise that comes from the continuous spectral component outside the gain bandwidth can

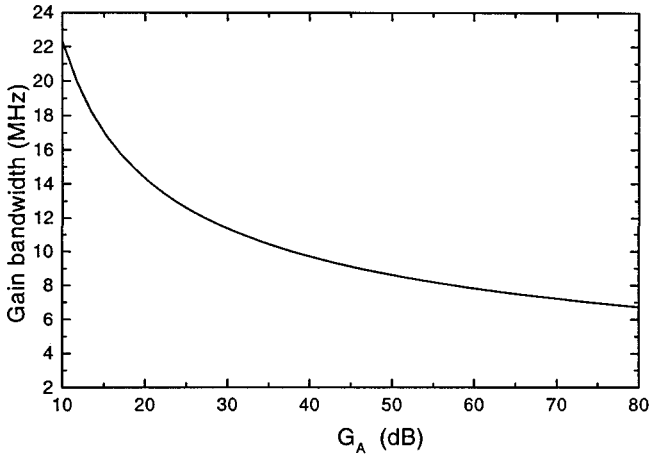

Fig. 4. SBS power gain bandwidth (FWHM) against line-center power gain $G_A(\Delta\nu_p \approx 0)$.

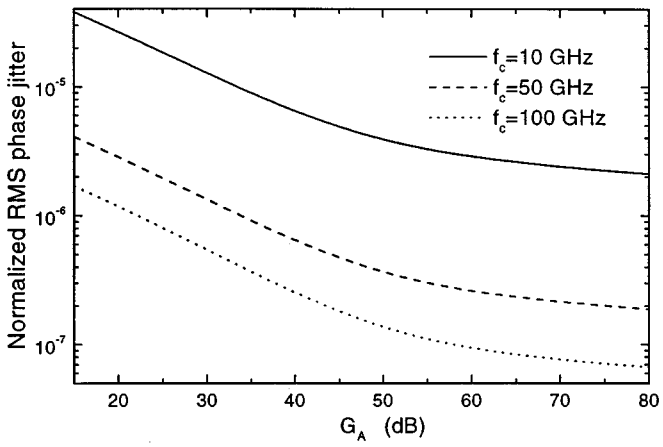

(a)

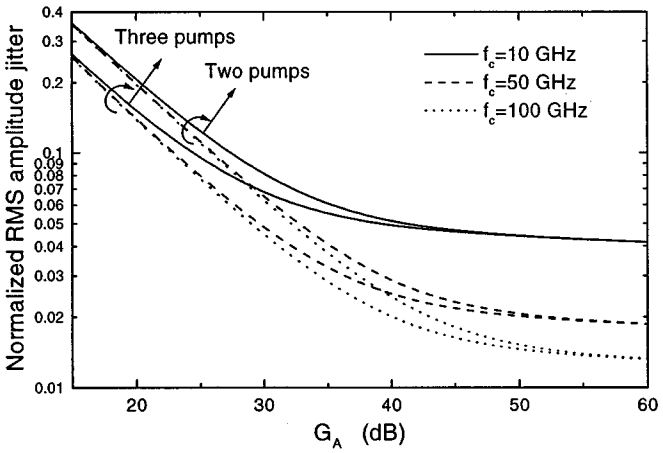

(b)

Fig. 5. Influence of SBS gain on (a) rms phase jitter and (b) rms amplitude jitter of the extracted optical clock for the case when $C = 0$, $\Delta f_k = 0$, and $\Delta\nu_p \approx 0$.

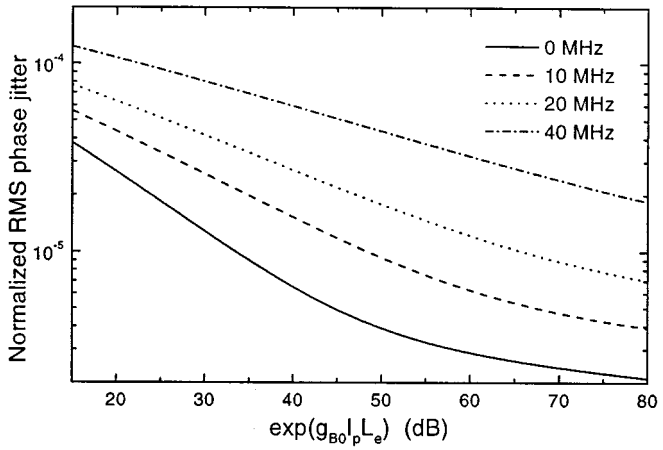

(a)

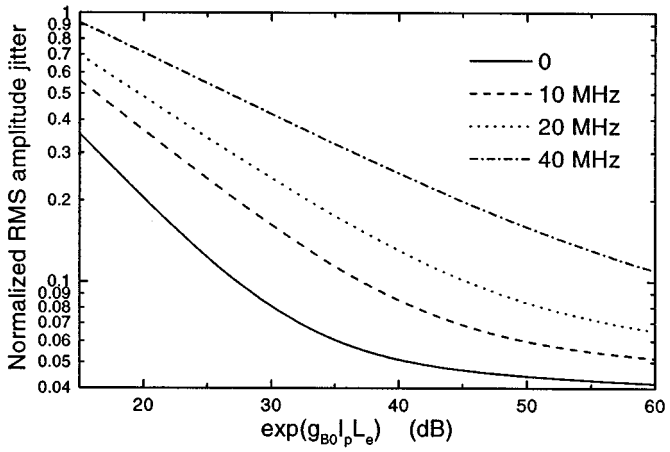

(b)

Fig. 6. Influence of pump light linewidth on (a) rms phase jitter and (b) rms amplitude jitter of the extracted optical clock. Two pump lights are used and we choose $C = 0$, $\Delta f_k = 0$, and $f_c = 10$ GHz. The solid, dashed, dot, and dashed-dot lines represent $\Delta\nu_p = 0$, 10, 20, and 40 MHz, respectively.

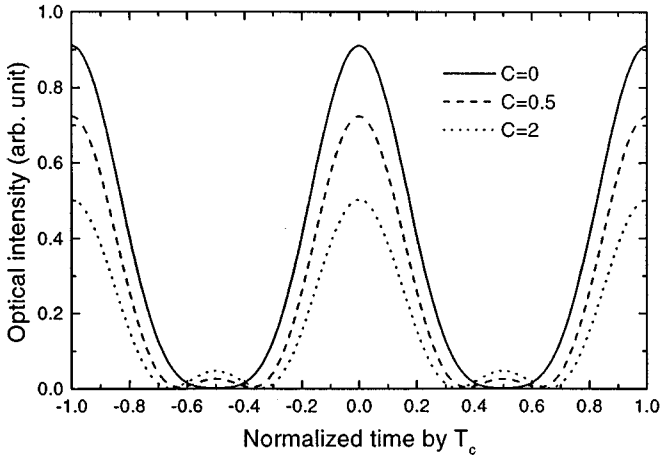

(a)

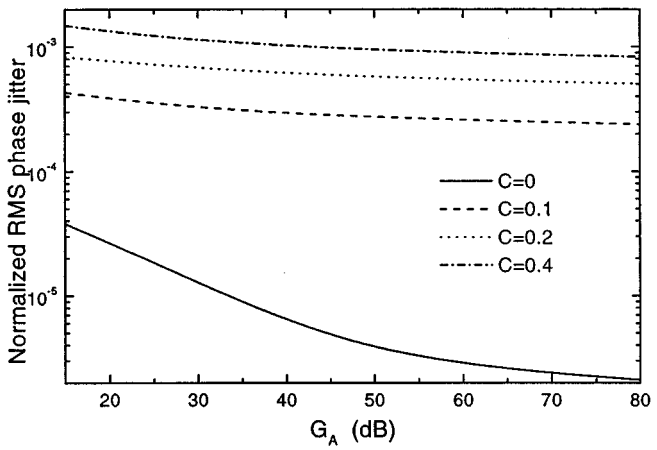

(b)

Fig. 7. Influence of optical pulse chirp on (a) average temporal profile (three pump lights are used) and (b) rms phase jitter of the extracted optical clock ($\Delta f_k = 0$, $\Delta\nu_p \approx 0$, $f_c = 10$ GHz, and $G_A = 30$ dB).

be much greater than that inside it and, therefore, becomes the dominate noise. In this situation, the impact of SBS gain and the number of pump lights become more serious than that of the quality factor (can be approximately viewed as the ratio of gain bandwidth to signal bit rate) of this circuit and they become the main factors to determine the value of σ_A. However, when G_A is large enough, the amplitude noise inside the gain bandwidth may become dominant; as a result, the ratio of gain bandwidth to signal bit rate becomes the main factor in the determination of amplitude jitter. From Fig. 4 we can see that the SBS gain bandwidth curve goes down very quickly when $G_A < 40$ dB, but slowly beyond this range. Accordingly, we can observe that σ_A tends to be a constant (denoted as σ_A^s hereafter) when $G_A >$ 40 dB. Note that σ_A^s is uniquely dependent on signal bit rate. For example, when signal bit rate is 10, 50, and 100 Gbs/s, the corresponding σ_A^s is 0.04, 0.02, and 0.014, respectively. This implies an upper bound for σ_A. As to σ_J, the phase noise always comes from the continuous spectral component inside the SBS gain bandwidth, therefore, the value of σ_J remains small for various values of G_A. Similarly to σ_A, we can find that, when G_A is large enough, σ_J tends to be a constant.

B. The Impact of Pump-Light Linewidth

Fig. 6(a) and (b) gives the calculated σ_J and σ_A against $\exp(g_{B0} I_p L_e)$ for various values of $\Delta\nu_p$ (Lorentzian spectral profile is assumed), respectively. Here we have assumed that pump depletion is negligible and used I_p to express the initial pump light intensity. It can be observed that both σ_J and σ_A increase as $\Delta\nu_p$ goes up. This is easy to understand, since the increase of $\Delta\nu_p$ will lead to an expansion in SBS gain bandwidth and a deduction in line-center gain.

C. The Impacts of Optical Pulse Chirp

During the process of obtaining (31), we have made an assumption that optical pulse chirp should be relatively small to ensure that $\arg[U(f_c)] - \arg[U(0)]$ remains small. In fact, even for large chirp, $\arg[U(f_c)] - \arg[U(0)]$ can still be small (for $C = 0.2$, 2, and 5, $\arg[U(f_c)] - \arg[U(0)]$ is estimated to be 0.044, 0.178, and 0.0855 rad, respectively). However, when the chirp is large, the spectrum of the optical pulse will broaden in a considerable degree and result in $B_0 < 2B_1$ (when optical pulse is very narrow, we have a similar result), thus a sidelobe will occur in the extracted optical clock pulse as shown in Fig. 7(a).

For two-pump clock extraction, we can see from (41) that the chirp will not introduce distortion of the clock pulse but will introduce an extra phase shift (equal to $\arg[U(f_c)] - \arg[U(0)]$) in the extracted optical clock. Our calculations also show that the introduction of optical pulse chirp will lead to an increase in rms phase jitter as shown in Fig. 7(b) (down-chirp has the same result as up-chirp), but impose nearly no impact on rms amplitude jitter.

D. The Impacts of Pump Detuning

To investigate the influence of pump detuning on timing performance, we assume $\Delta\nu_p \approx 0$ and choose $C = 0.2$.

1) Two Pumps with Two CW Lights: For the case that two-pump clock extraction with two independent CW lights, we have $\Delta f_0 = \Delta f_s + df_0$ and $\Delta f_1 = \Delta f_s + df_1$ as shown in Fig. 2. From (11) and (41), it is clear that unequal pump detuning will introduce an extra phase shift in the extracted optical clock. Due to the random nature of df_0 and df_1, this is equivalent to introducing a phase jitter, and implies that we need to control df_0 and df_1 to a rather small level. Typically, for negligible pump depletion and $G_A = 30$ dB, if we want the extra phase shift to be less than 0.1 rad, $|df_0|$ and $|df_1|$ must be lower than 0.25 MHz.

Now we turn to timing performance under systematic noise limit. Due to the smallness of df_0 and df_1, we can write $\Delta f_0 \approx \Delta f_s$ and $\Delta f_1 \approx \Delta f_s$. Figs. 8 and 9 give the calculated results. When pump depletion is neglected, we can see that σ_A, increase definitely with pump detuning for various SBS gains. However, this is not always true for the case that SBS gain is fully saturated. From Fig. 8(b) we can see that, when G_s is relatively small, σ_A will reduce as Δf_s increase so long as $|\Delta f_s|$ is within a critical value Δf_s^c. Note that Δf_s^c is dependent on G_s. For example, while $G_s = 20$, 30, and 40 dB, the corresponding Δf_s^c is estimated to be 7.5, 2.5, and 0 MHz, respectively. Unlike σ_A, we can see from Fig. 9 that the function curve of σ_J is asymmetrical, and the minimum value of σ_J does not occur at the point of $\Delta f_s = 0$ when $G_s < 40$ dB for both cases. Especially, we can see that the smaller G_s is, the smaller the minimum value of σ_J becomes.

Our calculation also shows that, so long as $|\Delta f_s| < 7.5$ MHz, $\sigma_A < 0.1$ and $\sigma_J < 0.01$ are obtainable (systematic noise limit). This implies that such a tank circuit can accept a carrier frequency variation of ± 130 GHz (based on (3) when $n = 1.44$ and $\nu_A = 5960$ ms^{-1}).

2) Three Pumps with One CW Light: For the case when three pumps are generated through a phase-modulated CW light, we have $\Delta f_0 = \Delta f_1 = \Delta f_{-1}$. The impact of pump detuning on σ_A is similar to the case when two pumps are used, as shown in Fig. 8. Calculations have shown that, if we require $\sigma_A < 0.1$, the acceptable carrier-frequency variation also need to be within ± 130 GHz. The impact of pump detuning on σ_J is shown in Fig. 10(a) and (b), where we have taken $f_c = 10$ GHz. We can see the curves are exactly symmetric and the minimum value of σ_J always occurs at the point of $\Delta f_0 = 0$ for various values of SBS gain. It is worth noting that the minimum value of σ_J decreases monotonously as SBS gain increases, this is different from the case where two pumps are used. From Fig. 10(b) we can also observe that, for the case when SBS gain is fully saturated, σ_J does not vary monotonously with pump detuning when G_s is large. For example, while $G_s = 40$ dB, we can observe that there exist three valley points occurring at $\Delta f_0 = 0$, 12, and -12 MHz, respectively. This can be supposed to be the impact

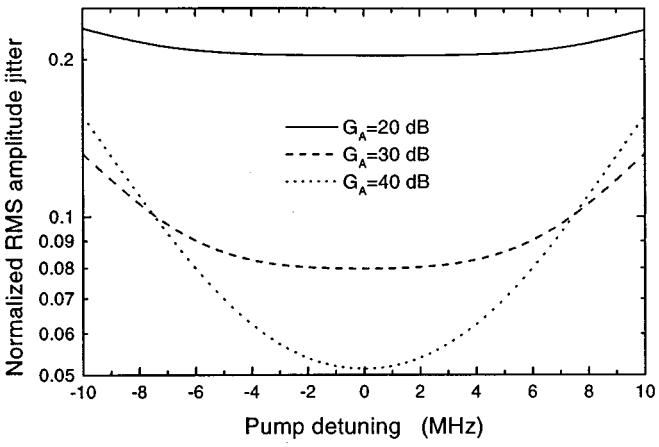

(a)

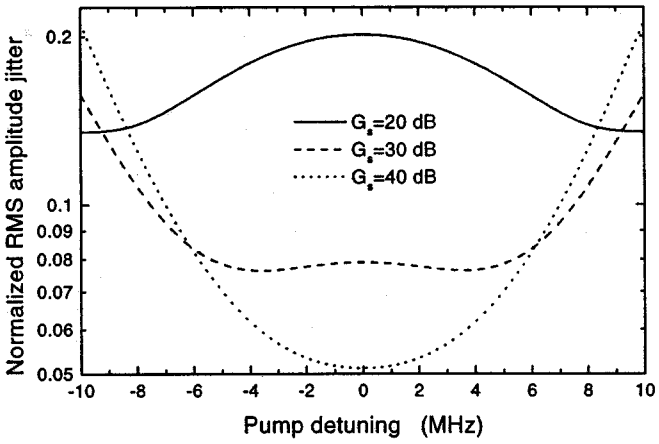

(b)

Fig. 8. Influence of pump detuning on rms amplitude jitter of the extracted clock (two pumps are used and $f_c = 10$ GHz). (a) Pump depletion is neglected. (b) SBS gain is fully saturated.

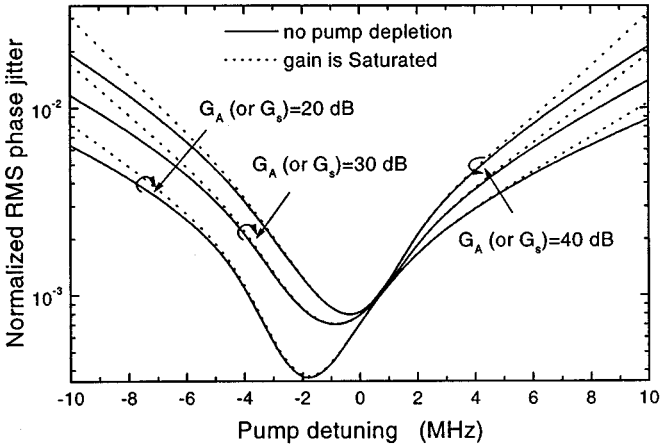

Fig. 9. Influence of pump detuning on rms phase jitter of the extracted optical clock (two pumps are used and $f_c = 10$ GHz).

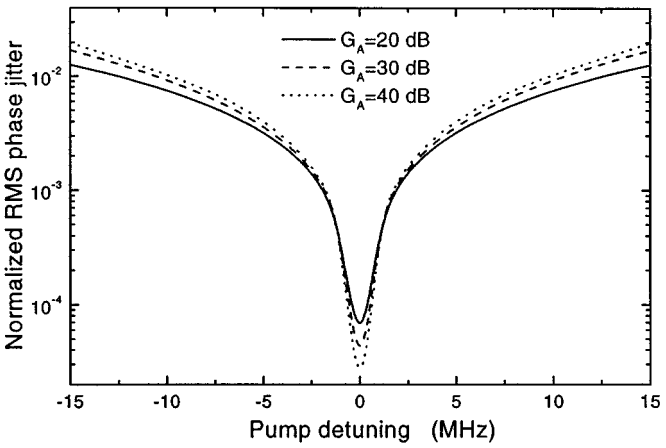

(a)

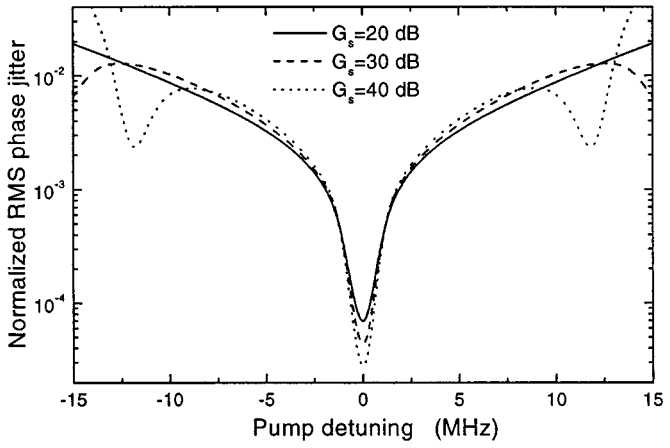

(b)

Fig. 10. Influence of pump detuning on rms phase jitter of the extracted clock for the case when three pumps are generated through a phase-modulated CW light. (a) Pump depletion is neglected. (b) SBS gain is fully saturated.

of the nonlinear phase shift Φ, since it is not limited to $\pm\pi/2$ as in the case of a linear single-pole tuned electronic amplifier. For example, for $G_s = 40$ dB, when $\Delta f_0 = 0$, 11.5, and -11.5 MHz, the nonlinear phase shift of the related signal line spectral components are estimated to be 0, 0.73π, and -0.73π, respectively.

Unlike the two-pump clock extraction scheme, we can see that AFC requirement on this scheme is less severe ($|\Delta f_s + \delta f| < 7.5$ MHz). However, its operating speed is limited by the electrical phase modulator.

3) Three Pumps Without Extra CW Light: As we know from the previous sections, in the case when pump lights are obtained directly from the signal, pump detuning δf includes two parts: inherent pump detuning and signal carrier-frequency variation-introduced detuning Δf_s. Note that δf is uniquely dependent on the signal bit rate ($\delta f \approx 5.7 \times 10^{-5} f_c$), therefore, we present the function curves of σ_A and σ_J against signal bit rate as shown in Fig. 11. It is worth noting that both σ_A and σ_J do not vary with signal bit rate monotonously, and multiple valley points occur in a curve. However, we can see that, when signal bit rate is above 300 Gbs/s, even $\Delta f_s = 0$, the value of σ_A will be greater than 0.1 and σ_J will be greater than 0.01 (though σ_J can be smaller by taking a small value of G_s, however, this will result in a degradation in σ_A). Consequently, the maximum operational rate is limited by the inherent pump detuning. From Fig. 11(b) and (d) we can also find that the acceptable signal carrier frequency variation is dependent on the signal bit rate. For f_c = 10, 100, and 300 Gbs/s, if we require $\sigma_A < 0.1$ and $\sigma_J < 0.01$, the allowable maximum carrier frequency variations are estimated to be $\pm$130 GHz, $\pm$100 GHz, and $\pm$18 GHz, respectively. This also implies that, if we use such a scheme for multiwavelength clock extraction, the allowable maximum wavelength span is about 2.1 nm ($f_c = 10$ GHz). Naturally, if we allow a larger rms amplitude jitter, such as 0.15, then the allowable maximum wavelength span can be 3.1 nm. Such a result agrees with the experiment in [9]. In fact, we can also increase the wavelength span by choosing a fiber with a larger SBS scattering linewidth.

Finally, we should point out that, the inherent pump detuning will introduce an extra phase shift $(\ln(G_s)\delta f/\Gamma)$ in the extracted clock.

VI. Conclusion

We have developed an analytical method to deal with the timing performance in an optical clock extraction circuit based on SBS. Three kinds of SBS active filters are considered and their frequency-transfer functions are obtained under the assumption that pump depletion caused by SBS is negligible. When pump depletion is taken into account, an SBS active filter acts as a nonlinear filter. To investigate the timing performance in this situation, we have introduced the concept of "dynamic frequency transfer function" to describe its frequency-response property for a fixed signal light and pump light. Using the obtained "frequency transfer function," we have given the analytical expressions for rms phase jitter and rms amplitude jitter of the extracted optical clock, in which we have taken the impacts of SBS gain, pump light linewidth, optical pulse chirp, and pump detuning into account. Finally, a detailed numerical investigation on the timing performance for the three active filters has been presented. Our results reveal the following.

1) In the case that no pump detuning occurs, both the rms phase jitter σ_J and rms amplitude jitter σ_A decrease as SBS gain goes up. For various values of SBS gain, σ_J remains very small but σ_A can be very large when line-center gain is less than 20 dB; such an effect is more serious for two-pump active filters. When SBS gain is over 40 dB, σ_A tends to be a constant which is uniquely dependent on SBS scattering linewidth and signal bit rate. σ_J has a similar effect but requires a larger value of the gain.
2) The increase of pump-light linewidth definitely degrades both σ_J and σ_A.
3) The introduction of the optical pulse chirp leads to an increase in σ_J but the impact on σ_A is very small.
4) Pump detuning is the main factor which degrades both σ_J and σ_A for the three active filters. Especially, in the case when pump lights are obtained directly from the signal, the inherent pump detuning imposes an upper bound (300 Gbs/s) on its operating speed.

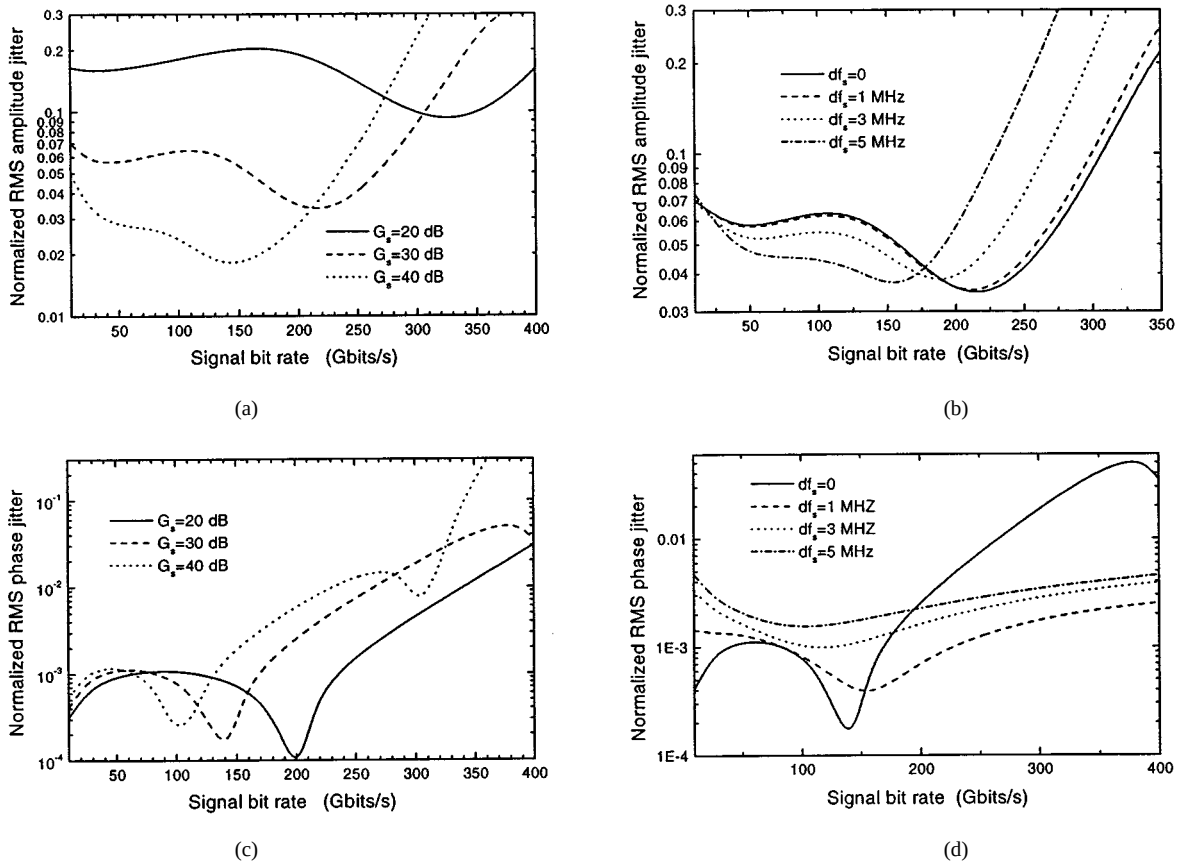

Fig. 11. Influence of the signal bit rate on rms amplitude jitter and rms phase jitter of the extracted optical clock for the case that three pumps are generated directly from the incoming signal. In (a) and (c) we take $\Delta f_c = 0$. In (b) and (d), we take $G_s = 30$ dB (the solid, dashed, dot, and dashed-dot denote the case when $\Delta f_s = 0$, 1, 3, 5 MHz, respectively).

APPENDIX
THE POWER SPECTRAL DENSITY OF THE EXTRACTED OPTICAL CLOCK

From (27), $R_{I,I}(t,\tau)$ can be expressed as

$$R_{I,I}(t,\tau) = \sum_{k_1=-\infty}^{\infty}\sum_{k_2=-\infty}^{\infty}\sum_{k_3=-\infty}^{\infty}\sum_{k_4=-\infty}^{\infty}\langle a_{k1}a_{k2}a_{k3}a_{k4}\rangle \cdot M(t,\tau,k_1,k_2,k_3,k_4) \quad (51)$$

where

$$M(t,\tau,k_1,k_2,k_3,k_4) = y(t-k_1T_c)y^*(t-k_2T_c)y(t+\tau-k_3T_c)y^*(t+\tau-k_4T_c)$$

and $y(t) = u(t) \otimes h(t)$. For convenience, we use $\Lambda(t,\tau)_{k_1,k_2,k_3,k_4}$ to represent

$$\sum_{k_1=-\infty}^{\infty}\sum_{k_2=-\infty}^{\infty}\sum_{k_3=-\infty}^{\infty}\sum_{k_4=-\infty}^{\infty} A(t,\tau,k_1,k_2,k_3,k_4).$$

Then $R_{I,I}(t,\tau)$ can be expressed as

$$\begin{aligned}R_{I,I}(t,\tau) &= \frac{1}{16}\underbrace{\Lambda(t,\tau)_{k_1,k_2,k_3,k_4}}_{k_1\neq k_2\neq k_3\neq k_4} \\ &\quad + \frac{1}{8}\underbrace{\Lambda(t,\tau)_{k_1,k_2,k_3,k_4}}_{\text{Three of } k_1,k_2,k_3,k_4 \text{ are unequal}} \\ &\quad + \frac{1}{4}\underbrace{\Lambda(t,\tau)_{k_1,k_2,k_3,k_4}}_{\text{Two of } k_1,k_2,k_3,k_4 \text{ are unequal}} \\ &\quad + \frac{1}{2}\Lambda(t,\tau)_{k_1,k_1,k_1,k_1} \\ &= \frac{1}{16}\Lambda(t,\tau)_{k_1,k_2,k_3,k_4} + \frac{1}{16}\{\Lambda(t,\tau)_{k_1,k_1,k_3,k_4} \\ &\quad + \Lambda(t,\tau)_{k_1,k_2,k_3,k_1} + \Lambda(t,\tau)_{k_1,k_2,k_2,k_4} \\ &\quad + \Lambda(t,\tau)_{k_1,k_2,k_3,k_2} + \Lambda(t,\tau)_{k_1,k_2,k_3,k_3}\} \\ &\quad + \frac{1}{16}\{\Lambda(t,\tau)_{k_1,k_1,k_2,k_2} + \Lambda(t,\tau)_{k_1,k_2,k_1,k_2} \\ &\quad + \Lambda(t,\tau)_{k_1,k_2,k_2,k_1}\} - \frac{1}{8} + \Lambda(t,\tau)_{k_1,k_1,k_1,k_1}.\end{aligned} \quad (52)$$

Note that

$$\Lambda(t,\tau)_{k_1,k_1,k_3,k_4} = \Lambda(t+\tau,-\tau)_{k_1,k_2,k_3,k_3}$$
$$\Lambda(t,\tau)_{k_1,k_2,k_2,k_4} = \Lambda^*(t,\tau)_{k_1,k_2,k_3,k_1}$$

and

$$\Lambda(t,\tau)_{k_1,k_2,k_1,k_4} = \Lambda^*(t,\tau)_{k_1,k_2,k_3,k_2}.$$

Assuming $\eta = f/f_c$ and using (48), the power spectral density

can be given as

$$
\begin{aligned}
S_I(\eta f_c) = \frac{f_c^4}{16} \sum_{k_1=-\infty}^{\infty} \Bigg\{ \sum_{k_2=-\infty}^{\infty} \sum_{k_3=-\infty}^{\infty} Y(k_2,k_1)Y(k_3,-k_1) \\
+ \sum_{k+2=-\infty}^{\infty} \Psi(-k_1)\left[Y(k_2,-k_1)+Y(k_2,k_1)\right] \\
+ \Psi(k_1)\Psi(-k_1) \Bigg\} \delta(\eta-k_1) \\
+ \frac{f_c^3}{16} \sum_{k_1=-\infty}^{\infty} \sum_{k_2=-\infty}^{\infty} \{Y^*(k_2-\eta,k_1)Y(k_2,k_1) \\
+ Y(k_2+\eta,k_1)Y^*(k_2,k_1) \\
+ Y^*(-k_2,-\eta)Y^*(k_1+k_2,\eta) \\
+ Y(-k_2,\eta)Y(k_1+k_2,-\eta)\} \\
+ \frac{f_c^3}{16} \sum_{k_1=-\infty}^{\infty} [\Theta_1(\eta,k_1)+\Theta_1(-k_1,\eta)] - \frac{f_c^3}{8}\Psi^2(-\eta)
\end{aligned}
\tag{53}
$$

where

$$
\begin{aligned}
Q(\eta) &= U(\eta f_c)\vec{H}_d(\eta f_c) \\
Y(\eta_1,\eta_2) &= Q(\eta_1)Q^*(\eta_2+\eta_1) \\
\Psi(\eta) &= \int_{\infty}^{\infty} Y(\eta',\eta)\,d\eta' \\
\Theta_1(\eta_1,\eta_2) &= \int_{-\infty}^{\infty} Y(\eta',\eta_1)Y(\eta_2-\eta',-\eta_1)\,d\eta'
\end{aligned}
$$

and

$$
\Theta_2(\eta_1,\eta_2) = \int_{-\infty}^{\infty} Y(\eta',\eta_1)Y^*(\eta_2+\eta',-\eta_1)\,d\eta'.
$$

Observing (53) carefully, we can find that the line spectral components in the second and third terms is small compared with the first term and the continuous spectral component in the final two terms is small compared with their previous four terms. Therefore, we can write $S_I(\eta f_c)$ in an approximate form as in (49).

REFERENCES

[1] L. Adams, E. Kintzer, and J. Fujimoto, "All-optical clock recovery using a mode-locked figure eight laser with a semiconductor nonlinearity," *Electron. Lett.*, vol. 30, p. 1696, Sept. 1994.

[2] R. Ludwig, "10 GHz all-optical clock recovery using a mode locked semiconductor laser in a 40 Gb/s, 100 km transmission experiment," in *OFC'96*, Mar. 1996, pp. 131–132.

[3] S. Kawanishi and M. Saruwatari, "Ultrahigh-speed PLL-type clock recovery circuit based on all-optical gain modulation in travelling-wave laser diode amplifier as a 50 GHz detector," *Electron. Lett.*, vol. 24, pp. 1714–1715, Sept. 1993.

[4] O. Kamatani and S. Kawanishi, "Ultrahigh-speed clock recovery with phase lock loop based on four-wave mixing in a traveling-wave laser diode amplifier," *J. Lightwave Technol.*, vol. 14, pp. 1757–1767, Aug. 1996.

[5] M. Jinno, T. Matsumoto, and M. Koga, "All-optical timing extraction using an optical tank circuit," *IEEE Photon. Technol. Lett.*, vol. 2, pp. 203–204, Feb. 1990.

[6] M. Jinno and T. Matsumoto, "Optical tank circuit used for all-optical timing recovery," *J. Quantum Electron.*, vol. 28, pp. 895–900, Apr. 1992.

[7] H. Kawakami, Y. Miyamoto, T. Katoka, and K. Hagimoto, "All-optical timing clock extraction using multiple wavelength pumped Brillouin amplifier," *IEICE Trans. Commun.*, vol. E78-B, pp. 694–700, May 1995.

[8] D. L. Butler, J. S. Wey, M. W. Chbat, G. L. Burdge, and J. Goldhar, "Optical clock recovery from a data stream of an arbitrary bit rate by use of Stimulated Brillouin Scattering," *Opt. Lett.*, vol. 20, pp. 560–562, June 1995.

[9] C. Johnson, K. Demarest, C. Allen, R. Hui, K. V. Peddanarappagari, and B. Zhu, "Multiwavelength all-optical clock recovery," *IEEE Photon. Technol. Lett.*, vol. 11, pp. 895–897, July 1999.

[10] X. Zhou, L. Chao, H. H. M. Shalaby, and P. Ye, "Performance analysis of an all-optical clock extraction circuit based on a Fabry-Perot resonator," J. Lightwave Technol., to be published.

[11] D. Cotter, D. W. Smith, C. G. Atkins, and R. Wyatt, "Influen ce of nonlinear dispersion in coherent narrowband amplification by stimulated Brillouin scattering," *Electron. Lett.*, vol. 22, pp. 671–672, Nov. 1986.

[12] R. W. Tkach, A. R. Chraplyyy, and R. M. Derosier, "Spontaneous Brillouin Scattering for single-mode optical-fiber characterization," *Electron. Lett.*, vol. 22, pp. 1011–1013, June 1986.

[13] G. P. Agrawal, *Nonlinear Fiber Optics*. London, U.K.: Academic, 1995, pp. 370–399.

[14] *Laser Handbook*, vol. 2, North Holland, Amesterdam, The Netherlands, 1972, pp. 1077–1150.

[15] M. O. Van Deventer and A. J. Boot, "Polarization properties of stimulated Brillouin Scattering in single-mode fibers," *J. Lightwave Technol.*, vol. 12, pp. 585–590, Apr. 1994.

[16] M. J. Rodwell, D. M. Bloom, and K. J. Weingarten, "Subpicosecond laser timing stabilization," *IEEE J. Quantum Electron.*, vol. 25, pp. 817–827, Apr. 1989.

[17] D. A. Leep and D. A. Holm, "Spectral measurement of timing jitter in gain-switched semiconductor lasers," *Appl. Phys. Lett.*, vol. 60, pp. 2451–2453, Oct. 1992.

[18] A. Buckwald and K. W. Martin, *Integrated Fiber-Optic Receiver*. New York: Kluwer, 1995, pp. 27–103.

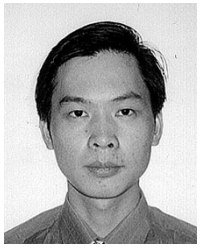

Xiang Zhou (M'00) was born in China. He received the B.Sc degree in applied physics from Shanghai Fudan University, Shanghai, China, in 1991 and the Ph.D. degree in optical fiber communication from Beijing University of Posts and Telecommunications, Beijing, China, in 1999.

After graduation he joined the Chinese Institute of Engineering Physics as an Assistant Researcher for three years. Currently, he is a Research Fellow at the Nanyang Technological University, working on technologies for wide-band optical amplifier, optical clock extraction, and photonic IP routing.

Hossam H. M. Shalaby (S'83–M'91–SM'99) was born in Giza, Egypt, in 1961. He received the B.S. and M.S. degrees from the University of Alexandria, Egypt, in 1983 and 1986, respectively, and the Ph.D. degree from the University of Maryland, College Park, in 1991, all in electrical engineering.

In 1991, he joined the Department of Electrical Engineering, University of Alexandria, as an Assistant Professor. He was promoted to Associate Professor in 1996. From March to April 1996, he was a Visiting Professor at the Electrical Engineering Department, Beirut Arab University, Lebanon. Since September 1996, he has been on leave from the University of Alexandria, where he was with two of the following places. From September 1996 to January 1998, he was an Associate Professor with the Electrical and Computer Engineering Department, International Islamic University Malaysia, and from February 1998 to December 1998, he was with the School of Electrical and Electronic Engineering, Nanyang Technological University, Singapore, where he was a Senior Lecturer, and since January 1999, an Associate Professor. His research interests include optical communications, optical CDMA, spread-spectrum communications, and information theory.

Dr. Shalaby was a recipient of an SRC Fellowship from 1987 to 1991 (System Research Center, MD), and both a State Award and Soliman Abd-El-Hay Award in 1995 (Academy of Scientific Research and Technology, Egypt). He served as a Chairman of the Student Activities Committee of Alexandria IEEE Subsection from 1995 to 1996. He also served as a Technical Referee for the *IEE Proceedings*, IEEE TRANSACTIONS ON COMMUNICATIONS, IEEE TRANSACTIONS ON INFORMATION THEORY, IEEE JOURNAL ON SELECTED AREAS IN COMMUNICATIONS, and the JOURNAL ON LIGHTWAVE TECHNOLOGY. He is listed in the 14th edition of *Marquis Who's Who in the World* in 1997.

Lu Chao (M'00) received the B.Eng. degree in 1985 from Tsing Hua University, Beijing, China, and the MSc and Ph.D. degrees from the University of Manchester Institute of Science and Technology(UMIST), U.K., in 1987 and 1990 respectively.

He joined the School of Electrical and Electronic Engineering, Nanyang Technological University, Singapore, in 1991, where he is currently an Associate Professor. His current research interests are in the area optical dense wavelength division multiplexing (DWDM) networks, fiber Bragg grating-based WDM devices, optical subcarrier multiplexing systems, and infrared wireless LANs.

T. H. Cheng (S'91–M'91) received the B.Eng. and Ph.D. degrees from the University of Stathclyde, U.K., in 1988 and 1992, respectively.

He is an Associate Professor in the Communication Engineering Division of the School of Electrical and Electronic Engineering. He holds the concurrent appointment of Director of Network Technology Research Centre since 1998. In 1994, he was appointed by Infocomm Development Authority (IDA) to serve in its Telecommunication Standards Technical Committee (TSTC), which formulates telecommunication standards for Singapore. He is a member of the Management Committee of the Singapore Advanced Research and Education Network (SingAREN) project jointly funded by the National Science and Technology Board (NSTB) and IDA. His main research interests include asynchronous transfer mode network and optical networking.

Peida Ye (F'88) was born in Shanghai in 1915. He graduated from Peiyang University, China, in 1938. From 1945 to 1946, he studied at Columbia University, New York.

He is now a Professor and Honorary President of Beijing University if Posts and Telecommunications, China. Currently, he is leading a research group working on ultrahigh-speed optical fiber communication systems and networks. He teaches a course at the graduate level on optical waveguide theory. He has published five books and more than 200 papers on electromagnetic theory, microwave theory, and optical communications.

Dr. Ye was elected as a member of the Chinese Academy of Science in 1980, and in 1990, was invited as a member of the Electromagnetic Academy of the Massachusetts Institute of Technology, Cambridge. In 1998, he was elected as a Governor of ICCC.